Surface Enhanced Raman Spectroscopy of Individual Rhodamine 6G Molecules on Large Ag Nanocrystals

Amy M. Michaels, M. Nirmal,† and L. E. Brus*

Contribution from the Department of Chemistry, Columbia University, New York, New York 10027

Received June 22, 1999

Abstract: To explore the relationship between local electromagnetic field enhancement and the large SERS (surface enhanced Raman scattering) enhancement that enables the observation of single molecule Raman spectra, we measure both resonant Rayleigh scattering spectra and rhodamine 6G Raman spectra from single Ag particles. Our apparatus combines the techniques of dark-field optical microscopy for resonant Rayleigh measurements, and grazing incidence Raman spectroscopy. The Rayleigh spectra show that the citrate-reduced Ag colloid is extremely heterogeneous. Only the larger particles, in part created by salt induced aggregation, show a large SERS effect. In agreement with the work of Nie and Emory, we find that a few nanocrystals show huge single molecule R6G SERS intensities. While all SERS active particles have some resonant Rayleigh scattering at the 514.5 nm laser wavelength, there is no correlation between the resonant Rayleigh spectra and the SERS intensity. We discuss a model in which huge SERS intensities result from single chemisorbed molecules interacting with ballistic electrons in optically excited large Ag particles. This model is a natural consequence of the standard local electromagnetic field model for SERS and the high surface sensitivity of plasmon dephasing in the noble metals.

Introduction

Molecular Raman scattering is a weak process, characterized by cross sections of $\sim 10^{-29}$ cm^2. Surface-enhanced Raman scattering (SERS) is commonly used to enhance Raman scattering intensities by up to 6 orders of magnitude.[1−4] In certain cases, though, the SERS enhancement can be enormous. In the 1980s, Pettinger et al.,[5] and Hildebrandt and Stockburger,[6] reported the Raman cross section of rhodamine 6G, at submonolayer coverage on aggregated Ag colloid, to be on the order of 10^{-16} cm^2 per molecule. In 1997, two groups independently reported SERS of single molecules adsorbed on Ag nanocrystals with similar cross sections.[7,8] These single molecule studies measured SERS enhancements of ∼14 orders of magnitude, demonstrating the potential to add a vibrational spectroscopy to the current methods for single molecule identification.

Despite extensive studies of SERS since its discovery nearly twenty-five years ago, and a literature consisting of thousands of papers, a complete understanding of the mechanism of enhancement is lacking. SERS has historically been described in terms of electromagnetic (EM) and chemical, or "first layer", enhancement mechanisms.[1−4] The relative importance of the two has remained ambiguous, as has the source of the chemical enhancement itself. The EM mechanism is based upon the optical properties of the noble metals Ag, Au, and Cu, and their ability to support plasmon resonances at visible wavelengths. Resonant excitation of surface plasmons creates an enhanced surface field $\mathbf{E}_S$ at both incoming and outgoing frequencies, resulting in an enhancement of the Raman signal that roughly scales as $(\mathbf{E}_S{}^4)$.[2,9] This mechanism does not require chemisorption and predicts equal enhancements for all molecules. $\mathbf{E}_S$ can be calculated from Maxwell's equations and, in general, maximum enhancement factors of $\sim 10^6-10^7$ are predicted.[10−16]

Certain experiments provide evidence for a chemical enhancement mechanism. For example, CO and N_2 have nearly identical free space Raman scattering cross sections, yet the SERS spectrum of CO is nearly 2 orders of magnitude stronger than that of N_2.[17] In addition, for CO, which exists in both chemisorbed and physisorbed forms on rough Ag surfaces, the chemisorbed species yields a larger SERS signal.[1] Consistent with these observations, SERS may result from a resonant scattering process due to an adsorption-induced metal-to-molecule or molecule-to-metal charge-transfer electronic transition.[1,18] Alternatively, it is possible that the enhancement results

† Present address: 3M, St. Paul, MN 55144.

(1) Otto, A.; Mrozek, I.; Grabhorn, H.; Akemann, W. *J. Phys.: Condens. Mater*. **1992**, *4*, 1143−1212.
(2) Moskovits, M. *Rev. Mod. Phys*. **1985**, *57*, 783−826.
(3) Schatz, G. *Acc. Chem. Res.* **1984**, *17*, 370−376.
(4) Campion, A. *Chem. Soc. Rev*. **1998**, *4*, 241−250.
(5) Pettinger, B.; Krischer, K.; Ertl, G. *Chem. Phys. Lett*. **1988**, *151*, 151−155.
(6) Hildebrandt, P.; Stockburger, M. *J. Phys. Chem*. **1984**, *88*, 5935−5944.
(7) Nie, S.; Emory, S. R. *Science*. **1997**, *275*, 1102−1106.
(8) (a) Kneipp, K.; Wang, Y.; Kneipp, H.; Perelman, L. T.; Itzkan, I.; Dasari, R. R.; Feld, M. S. *Phys. Rev. Lett*. **1997**, *78*, 1667−1670. (b) Kneipp, K.; Kneipp, H.; Deinum, G.; Itzkan, I.; Dasari, R. R.; Feld, M. S. *Appl. Spectrosc.* **1998**, *52*, 175−178. (c) Kneipp, K.; Kneipp, H.; Kartha, B.; Manoharan, R.; Deinum, G.; Itzkan, I.; Dasari, R. R.; Feld, M. S. *Phys. Rev. E*. **1998**, *57*, R6281−R6284.
(9) Metiu, H.; Das, P. *Annu. Rev. Phys. Chem*. **1984**, *35*, 507−536.
(10) Kerker, M.; Wang, D.; Chew, H. *Appl. Opt*. **1980**, *19*, 4159−4173.
(11) Barber, P. W.; Chang, R. K.; Massoudi, H. *Phys. Rev. B.* **1983**, *27*, 7251−7261.
(12) Creighton, J. A. In *Surface Enhanced Raman Scattering*; Chang, R. K., Furtak, T. E., Eds.; Plenum Press: New York, 1982; pp 315−337.
(13) Gersten, J.; Nitzan, A. *J. Chem. Phys*. **1980**, *73*, 3023−3037.
(14) Garcia-Vidal, F. J.; Pendry, J. B. *Phys. Rev. Lett*. **1996**, *77*, 1163−1166.
(15) Zeman, E. J.; Carron, K. T.; Schatz, G. C.; Van Duyne, R. P. *J. Chem. Phys*. **1987**, *87*, 4189−4200.
(16) Yang, Y.; Schatz, G. C.; Van Duyne, R. P. *J. Chem. Phys*. **1995**, *103*, 869−875.
(17) Moskovits, M.; DiLella, D. P. in *Surface Enhanced Raman Scattering*; Chang, R. K., Furtak, T. E., Eds.; Plenum Press: New York, 1982; pp 243−273.

10.1021/ja992128q CCC: $18.00
Published on Web 10/14/1999

from the interaction of chemisorbed molecules with ballistic ("hot") electrons that are generated through plasmon excitation.[19,20] Quantitative estimates of chemical enhancement factors have ranged from a factor of 10−100.

A key obstacle in determining the relative importance of the electromagnetic versus the chemical enhancement mechanism is the fact that the two are inextricably linked in strong SERS. In an effort to separate these mechanisms, we have independently measured both the SERS enhancement and the EM plasmon scattering enhancement for single rhodamine 6G (R6G) molecules adsorbed on individual Ag nanocrystals. This system has been characterized in detail by several groups in both ensemble and single molecule experiments.[5−7] We have used resonant Rayleigh scattering to probe the electromagnetic resonances of the Ag particles. If the surface plasmon resonance were the only necessary factor for Raman enhancement, then all SERS-active particles should have a strong resonance in their scattering spectrum at the SERS excitation frequency.

Prior studies that have examined the correlation between the surface plasmon resonance of Ag colloids and the SERS signal have relied upon ensemble measurements. However, these colloids are extremely heterogeneous. Since scattering spectra are explicitly dependent upon the shape and size of a particle, the resonant Rayleigh spectrum of each particle in such a distribution is expected to be quite different. The experiments reported here probe the specific, individual Ag nanocrystals that yield SERS by measuring their individual scattering spectra using the technique of dark-field microscopy. Since only certain Ag nanocrystals yield strong SERS, comparisons can be made between SERS-active and SERS-inactive nanocrystals. Our results indicate that while some EM enhancement is necessary to detect SERS of single R6G molecules, there is no correlation between the SERS intensity and the resonant Rayleigh spectra of the SERS-active particle. We discuss our results in terms of the interaction of ballistic electrons in the nanocrystal with chemisorbed molecules, which has been previously considered by Otto and Persson.[19,20]

Experimental Section

Reagents and Materials. Silver nitrate was obtained from Aldrich. Sodium citrate, poly-L-lysine, and sodium chloride were purchased from Sigma. R6G was obtained from Exciton, and DiI (1,1′-didodecyl-3,3,3′,3′-tetramethylindocarbocyanine) from Molecular Probes. All reagents were used as received. Aqueous solutions were prepared using distilled deionized water.

Sample Preparation. Colloidal Ag nanoparticles were prepared in aqueous solution following the procedure of Lee and Meisel.[21] $AgNO_3$ (54 mg) was dissolved in hot water (∼40 °C), and heated with vigorous stirring. Upon boiling, a 1% solution of sodium citrate (6 mL) was added rapidly. The solution was refluxed for approximately 90 min. The absorption spectrum of the resulting brownish solution was typically characterized by a maximum at ∼408 nm and a fwhm of ∼110 nm.

For sample preparation, we followed the general procedures of Nie and Emory.[7,22] An aliquot of the Ag colloid was diluted by a factor of 3, and a sample was prepared by spin-coating one drop of diluted colloid onto a polylysine-coated quartz cover slip. To examine the effect of salt, an aliquot of the colloid was incubated with 1 mM, 10 mM, or 30 mM NaCl under ambient conditions prior to spin-coating. After spin-coating, cover slip samples were rinsed with water to remove any NaCl particles. For optical studies, these samples were used immediately. Samples were prepared similarly for AFM experiments, but were dried overnight before use.

For SERS studies, an aliquot of diluted Ag colloid was incubated with the specified concentration of salt under ambient conditions. R6G was then added to yield a concentration of 8×10^{-10} M, unless otherwise noted. After a 20 min incubation period at room temperature, one drop of the Ag/R6G solution was spin coated onto a polylysine-coated quartz cover slip.

To calibrate the SERS signal intensity, DiI samples were prepared by spin-coating one drop of a 0.5% PMMA solution onto a quartz cover slip, followed by one drop of a 5×10^{-10} M DiI solution.

Atomic Force Microscopy (AFM) Imaging. A Nanoscope IIIA scanning probe microscope (Digital Instruments) was used in tapping mode to obtain AFM images of the Ag samples under ambient conditions.

Resonant Rayleigh Imaging and Spectroscopy. Scattering images and spectra were obtained using an inverted optical microscope (Eclipse TE300, Nikon Instruments) equipped with a dark-field condenser and a tungsten lamp. Scattered light was collected by a microscope objective (Nikon, Plan Fluor, 100× oil; or Nikon, ELWD, 50×, NA = 0.55, air) and focused onto the entrance slit of a spectrometer (Spex 270M, Instruments SA) using a camera lens (Nikon). A liquid nitrogen-cooled CCD camera (Princeton Instruments) recorded both images and scattering spectra.

The spectrometer is equipped with a dual mirror-grating turret which allows one to switch between imaging and spectroscopy modes. By using the mirror and opening the slits to their maximum 7 mm width, a 120 μm × 150 μm field of view is imaged onto the CCD camera. To obtain spectra of single Ag nanoparticles, individual scattering spots were centered on the entrance slit of the spectrometer by moving the sample on a piezoelectric driven stage. The entrance slit was narrowed and the grating (300 g/mm; 500 nm blaze) was rotated into the optical path. All spectra were corrected to account for the spectral variation of the tungsten lamp.

SERS Imaging and Spectroscopy. For SERS measurements, the sample was irradiated with ∼35 mW of 514.5 nm laser light (Innova 308, Coherent) at an 80 degree angle of incidence. The illuminated area was ∼150 μm × 1 mm, yielding a power density of ∼30 W/cm^2. A holographic notch filter (Kaiser Optical) in front of the spectrometer entrance slit blocked the Rayleigh scattered light. Images and spectra were acquired as described above. All light that is Stokes-shifted by more than 500 cm^{-1} was recorded.

To correlate the SERS spectra with the corresponding resonant Rayleigh spectra, the SERS-active particles were first identified. The tungsten lamp Rayleigh scattering spectrum of the corresponding particle was then recorded after removing the notch filter from the detection path. Finally, a monochromatic Rayleigh scattering image of SERS-active particles was acquired using the 514.5 nm laser excitation.

Results

AFM Characterization. A tapping mode AFM image shown in Figure 1 shows the polydispersity and average size of the Ag colloidal particles without NaCl incubation. The colloid consists of single particles of varying shapes, sizes, and aspect ratios, including both smaller spherical and long rod-shaped particles. There are very few aggregates. The average particle size, as determined by the average maximum height is ∼55 nm. There is evidence of some aggregation with the addition of 1 mM NaCl. Most particles, though, are single nanocrystals. AFM images of Ag nanoparticles incubated with 10 mM NaCl provide clear evidence of aggregation, although some single particles still remain. The aggregates are compact combinations of primarily four, five, and six individual nanocrystals, forming composite particles of low symmetry, and ranging from ∼120 to 250 nm in size. We do not observe any open, fractal-like aggregates.

(18) (a) Lombardi, J. R.; Birke, R. L.; Lu, T.; Xu, J. *J. Chem. Phys.* **1986**, *84*, 4174−4180. (b) Kambhampati, P.; Child, C. M.; Foster, M. C.; Campion, A. *J. Chem. Phys.* **1998**, *12*, 5013−5026.

(19) Otto, A. in *Light Scattering in Solids IV*; Cardona, M., Gundtherodt, G., Eds.; Springer-Verlag: Berlin, 1984; pp 289−418.

(20) Persson, B. N. J. *Chem. Phys. Lett.* **1981**, *82*, 561−565.

(21) Lee, P. C.; Meisel, D. *J. Phys. Chem.* **1982**, *86*, 3391−3395.

(22) (a) Emory, S. R.; Haskins, W. E.; Nie, S. *J. Am. Chem. Soc.* **1998**, *120*, 8009−8010. (b) Emory, S. R.; Nie, S. *J. Phys. Chem. B.* **1998**, *102*, 493−497.

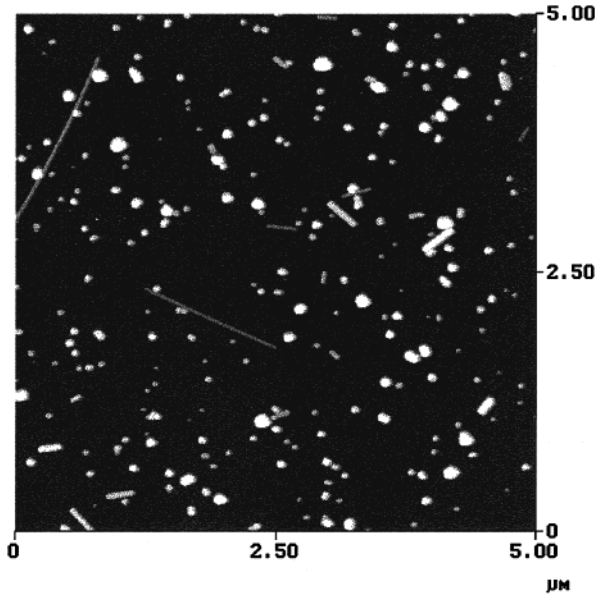

Figure 1. AFM image of Ag nanocrystals without NaCl incubation.

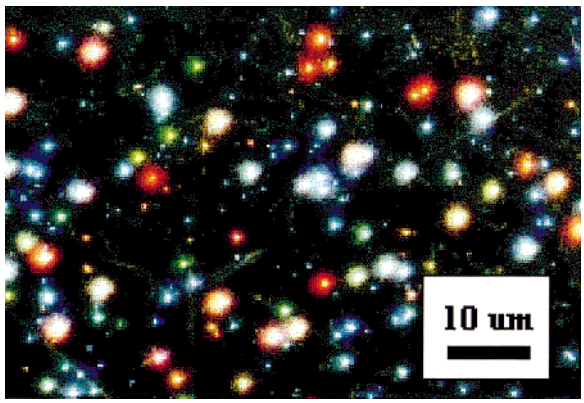

Figure 2. Single Ag nanocrystals incubated with 1 mM NaCl and imaged using dark-field microscopy. The image was recorded on color photographic film with a 20 s exposure using a Nikon 35 mm camera. Certain particles scattered very brightly and appear overexposed in order to image the particles that scatter less strongly. The lines in the image resulted from scattering from the scratches on the quartz cover slip.

Resonant Rayleigh Scattering. Figure 2 shows a tungsten lamp resonant Rayleigh image of individual Ag nanocrystals without NaCl incubation. Due to the polydispersity of the sample, different particles have both different scattering resonances and intensities. Examples of resonant Rayleigh spectra of individual Ag particles are shown in Figure 3a. Almost all spectra from this sample are characterized by a single peak with a fairly large (∼100 nm fwhm) line width. A commonly observed spectrum has a single blue peak (400−450 nm), which, in Mie theory, corresponds to a spherical Ag nanocrystal with a radius of ∼50 nm. However, these particles are, in general, not spherical, and significantly smaller particles characterized by axial ratios greater than one will also scatter at these wavelengths. The spectra characterized by red resonances correspond to particles with very high axial ratios, such as the long rods seen in the AFM images. There are occasionally more complex spectra, as shown in Figure 3b, however such examples account for less than 10% of the scattering spectra acquired. Comparison with AFM images suggests that these complex scattering spectra correspond to the small percentage of aggregates in the sample.

The colloidal extinction spectrum in Figure 4 shows essentially no change with the addition of salt. However, with increasing quantities of salt, the probability of obtaining complex resonant Rayleigh spectra, as in Figure 3b, increases due to aggregation of the Ag particles. The addition of 1mM NaCl slightly increases the probability that a scattering signal will yield a complex spectrum. This probability increases to more than 50% with the addition of 30 mM NaCl.

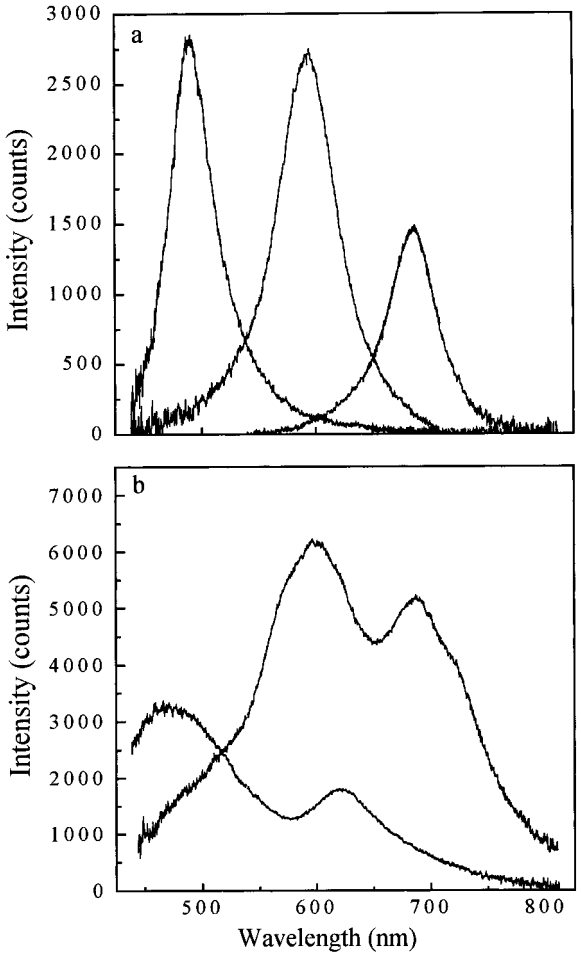

Figure 3. (a) Typical resonant Rayleigh spectra for arbitrarily selected Ag particles obtained using dark-field microscopy. (b) Examples of complex resonant Rayleigh spectra observed for <10% of Ag nanocrystals studied without the addition of NaCl. Spectra were obtained with a 10 s integration time.

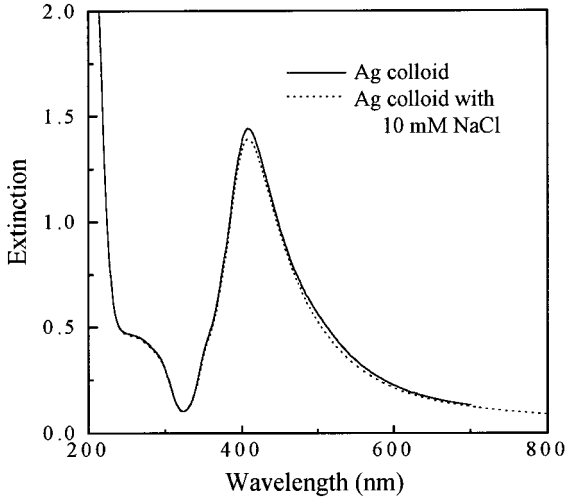

Figure 4. Extinction spectrum of the Ag colloid with and without 10 mM NaCl.

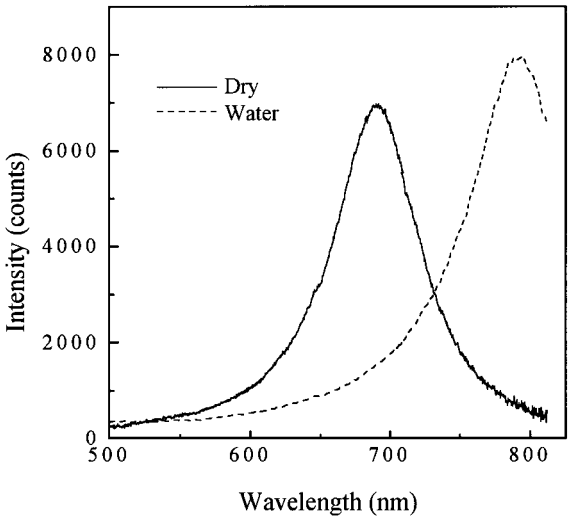

Figure 5. Resonant Rayleigh scattering spectra of a single Ag particle in air and in water.

In Mie theory, increasing the refractive index of the surrounding medium shifts the peak of the plasmon resonance to lower frequency. As shown in Figure 5, a water layer ~500−1000 μm thick on top of a dry Ag sample shifted the plasmon resonance by more than 100 nm, yet did not cause any apparent change in the shape or width of the spectrum. This shift was reversible upon drying. Even greater shifts were obtained with an immersion oil ($n = 1.47$) film.

Surface-Enhanced Raman Scattering. At concentrations of 8×10^{-10} M R6G and 1 mM NaCl, less than 0.1% of Ag nanocrystals yield detectable SERS signals. Statistically, there are about 2 R6G molecules per Ag nanocrystal at this concentration, based upon estimates given by Emory and Nie.[7] With 10 mM NaCl, the percentage of SERS-active particles increases to ~1%. Additional increases in salt concentration up to 30 mM resulted in further increases in the number of SERS-active particles, suggesting that aggregates are responsible for the large SERS enhancement.

The effect of the concentration of R6G on the SERS signal was examined by preparing samples with R6G concentrations varying from 8×10^{-10} to 1×10^{-7} M. The intensity of the SERS signal from one nanocrystal did not significantly increase with additional R6G. Rather, the number of SERS-active Ag nanocrystals increased. However, the percentage of SERS active particles did not increase linearly with R6G concentration. At 10 mM NaCl, a 125-fold increase in the concentration of R6G increased the number of SERS-active particles by a factor of ~5. At all concentrations, though, the SERS active particles showed "blinking", characterized both by on/off behavior and variations in integrated intensity, as shown in Figure 6.

The magnitude of the SERS cross section was measured by taking the ratio of the SERS count rate against the fluorescence count rate for single DiI molecules (without Ag particles) under the same experimental conditions. Using an absorption cross section for DiI fluorescence of 1.3×10^{-16} cm^2 at 514.5 nm,[23] the SERS cross sections show a wide distribution with an average of 2×10^{-14} cm^2 for a sample of 101 active SERS particles (Figure 7). Overall, our data is consistent with the results of Nie and Emory; however, our average cross section is somewhat higher than their approximate value.[7]

An example of an R6G SERS spectrum is shown in Figure 8. The marked peaks correspond to the Raman lines for R6G.

(23) Macklin, J. J.; Trautman, J. K.; Harris, T. D.; Brus, L. E. *Science* **1996**, *272*, 255−258.

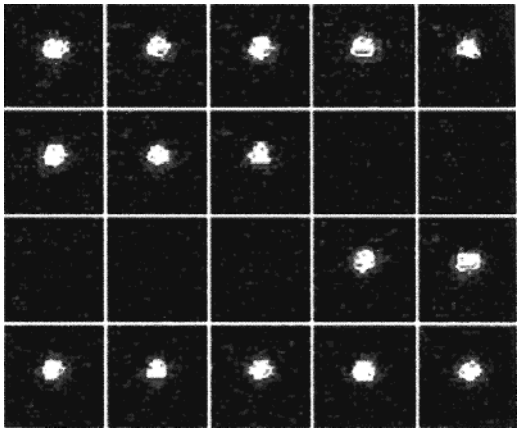

Figure 6. Intermittent SERS signal from R6G adsorbed on a single Ag nanoparticle. The integration time per frame is 1 s, and the rate of acquisition is 0.5 Hz. For this particle, the peak intensity for the "on" time is ~150 cps. When the particle blinks "off", this intensity drops to ~1 cps (the background count rate).

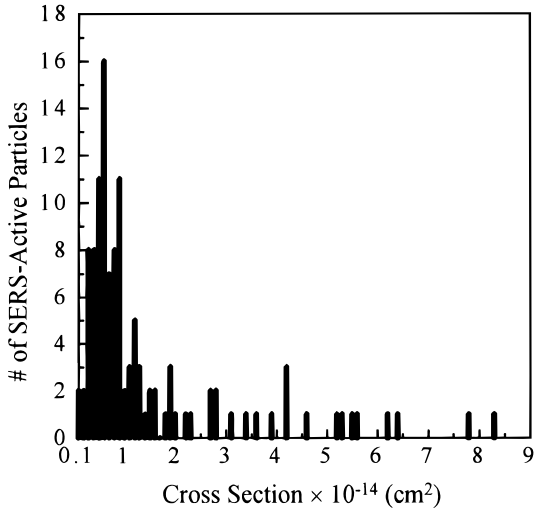

Figure 7. Distribution of measured cross sections for R6G SERS obtained by taking the ratio of counts for SERS emission to single molecule DiI emission, as described in the text. Particles with an effective cross section of less than 10^{-15} cm^2 were not recorded .

The broadband white continuum underneath the Raman lines is present in every SERS spectrum that we recorded. This continuum varies in intensity, in shape, and as a function of time for a single particle, and generally contributes the majority of the total measured SERS signal. This strong continuum emission only appears in conjunction with the R6G Raman signal; when the Raman signal blinks off, so does the continuum. Conversely, when the Raman signal reappears, the continuum does as well.

We do not observe strong SERS from small Ag particles with plasmon resonances in the blue. All SERS active Ag nanocrystals are characterized by either strong or weak resonant Rayleigh scattering at 514.5 nm (the SERS excitation wavelength). However, there is no apparent common feature to these spectra. The Rayleigh spectra of these particles all show a high degree of complexity, with a minimum of two scattering peaks for each spectrum. There is a wide scatter between the intensity of the SERS signal and the Rayleigh scattering intensity, as shown in Figure 9. Additionally, there are many nanocrystals that strongly scatter at 514.5 nm, but do not show strong SERS. Altering the dielectric constant of the surrounding medium with either water or oil resulted in no net effect on the SERS signal.

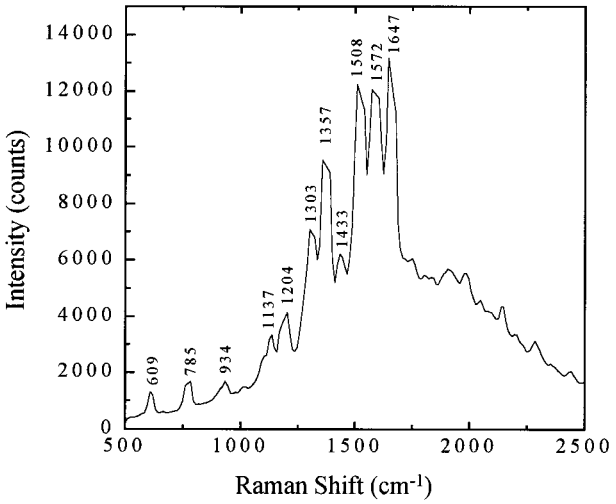

Figure 8. SERS spectrum for R6G adsorbed on a single Ag nanoparticle. NaCl was added at a concentration of 1 mM, and R6G was added at a concentration of 7×10^{-10} M. The integration time was 60 s at ~30 W/cm^2. The spectral resolution is 50 cm^{-1}. The Raman line widths are instrument-limited.

We also compared the 514.5 nm Rayleigh signal of the SERS-active particles with the strength of the SERS signal. No correlation was observed. Figure 10 presents a scatter plot of the scattered Rayleigh intensity versus the R6G SERS intensity for 35 SERS-active particles. Particles with comparable Rayleigh signals yielded significantly varying SERS signals. On average, the 514.5 nm Rayleigh signal was ~6000× stronger than the Raman scattering. Since calculated cross sections for Rayleigh scattering for spheroidal and ellipsoidal particles in the relevant size regime are of the order of 10^{-10} cm^2, these results very roughly corroborate the large magnitude of the measured SERS cross section.

Discussion

Analysis of Data. No two Ag particles have identical resonant Rayleigh scattering spectra. This diversity is not apparent in the colloidal (ensemble) extinction spectrum, which shows a single broadened peak in the blue. Mie calculations show that slightly ellipsoidal particles with a major axis of ~50 nm, which dominate the sample as characterized in our AFM images, have an extinction peak at ~400 nm and are characterized by an optical absorption cross section comparable to the scattering cross section. For the larger 100−200 nm rodlike particles and the compact aggregates of similar size formed by salt addition, the extinction cross section is dominated by Rayleigh scattering. Therefore, in an extremely heterogeneous sample containing many smaller ellipsoidal particles and a few larger particles, the extinction spectrum is likely to be dominated by the many smaller particles and the Rayleigh scattering spectrum by the few larger particles.

In large particles, the calculated Rayleigh scattering cross section is typically 1−10× the geometrical cross section. For particles ~100 nm in size, Mie theory predicts a scattering cross section of 10^{-10} cm^2. Thus, a 100 nm Ag particle is a huge mesoscopic dipole that scatters initial plane wave laser radiation incoherently in all directions, and the resonant peaks observed in the far-field Rayleigh scattering spectrum necessarily correspond to $\mathbf{E}_S$ enhancement near the particle.

We observe no correlation between the R6G SERS signal and the resonant Rayleigh scattering spectra of the corresponding Ag particle. Furthermore, there are many particles that show a strong Rayleigh resonance at 514.5 nm, yet no SERS scattering, despite the fact that statistically, there are about 2 R6G molecules per particle. We therefore conclude that $\mathbf{E}_S$ alone is not the sole critical factor in yielding the enormous SERS enhancement that we observe.

Following the earlier ideas of Otto, Persson, and others, we propose that strong chemisorption is also required for a large Raman scattering. As the number of particles that yield strong SERS is <1%, and increases highly sublinearly with R6G concentration, these special chemisorption sites are quite rare. Under the conditions of our present experiment, there appears to be less than one such site per particle. Our results are similar to those of the 1984 liquid-phase studies of Hildebrandt and Stockburger. They also concluded strong chemisorption at special sites which are activated by the addition of 1 mM chloride ions is necessary for SERS. The enormous Raman

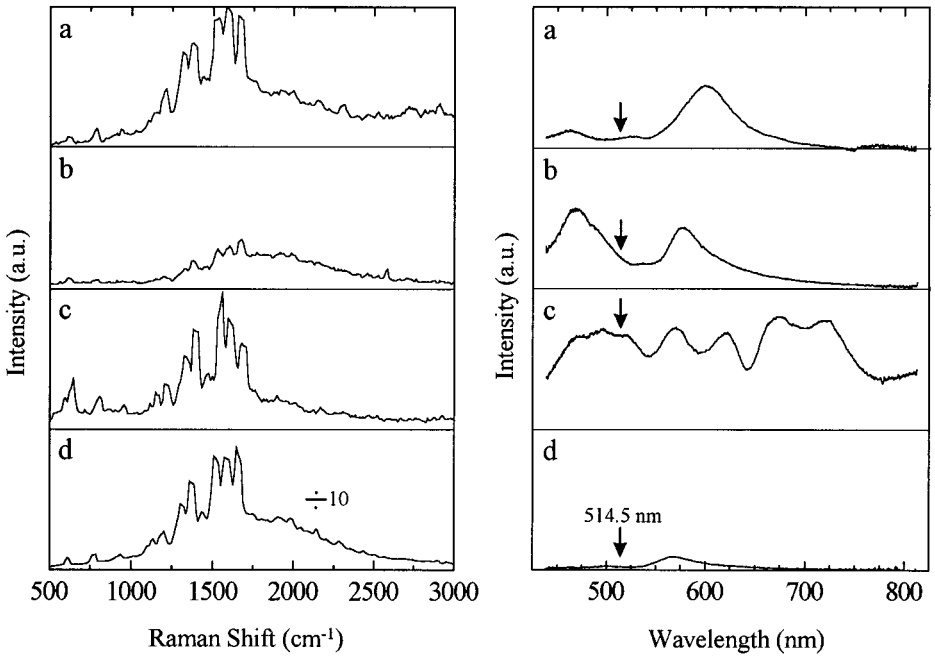

Figure 9. Corresponding R6G SERS (left) and resonant Rayleigh (right) spectra from four individual Ag nanoparticles.

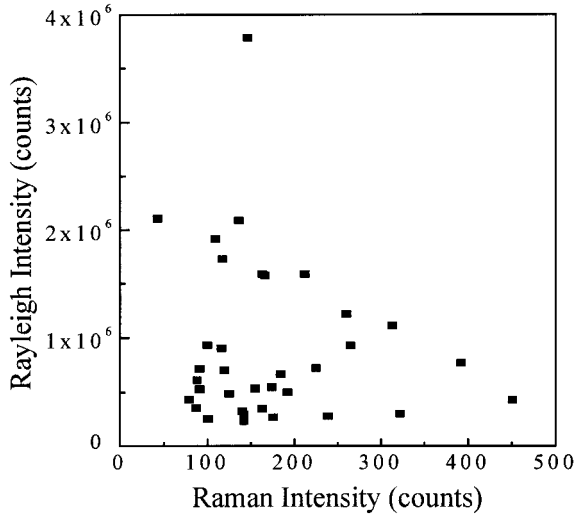

Figure 10. Scatter plot of the 514.5 nm Rayleigh signal to R6G SERS signal for 35 SERS-active individual Ag nanoparticles. The average Rayleigh signal is approximately 6000× stronger than the corresponding Raman signal.

signal from R6G chemisorbed at these special sites saturated at 10^{-9} M added R6G![6]

In the simple field enhancement model (without required chemisorption), the effective Raman cross section is obtained by multiplying the unperturbed Raman cross section by the local field enhancement factor. Theory predicts that local field enhancement factors can be as high as 10^7 for the smaller Ag particles (<30 nm) and systematically decrease with increasing size.[11] Particles that are ~100 nm in size, characteristic of the SERS-active particles in our work, should have a small $\mathbf{E}_S$ enhancement. The strong single molecule SERS that we observe is therefore not consistent with the model of simple field enhancement, even for adsorbed molecules. It is true that R6G is electronically resonant as a solute in water at 514.5 nm. Yet, we do not detect Raman signals for all R6G molecules present. Furthermore, we do not observe a Raman signal from the citrate ion which is known to cover the surface of these particles, the polylysine on the quartz substrate, or any residual water in the sample. It should be noted, though, that under the current experimental conditions, we do not detect signals that are 20× weaker than observed for R6G.

Our results also suggest that the underlying white continuum in the SERS spectrum is directly related to the enhanced molecular Raman signal. Many SERS studies have reported this continuum, which is not present in Raman scattering spectra of unperturbed molecules. We have observed that this continuum is never present without the R6G signal, yet it appears in every SERS spectrum that we recorded. Furthermore, the two signals blink on and off together. R6G chemisorption may be the factor that triggers both the continuum emission and R6G Raman enhancement. If we model the blinking as a thermal (or laser driven) desorption and readsorption of R6G from one site, then desorption of R6G would shut off both signals, while readsorption would reactivate the signal.

Local Field Enhancement and Ballistic Electron−Hole Pairs. Consider an electromagnetic field $\mathbf{E}(\omega)$ interacting with a small sphere of radius a and complex dielectric constant $\epsilon = \epsilon' + i\,\epsilon''$ in a vacuum. In the electrostatic limit without retardation, the electromagnetic field inside the sphere, $\mathbf{E}_{in}$, is

$$\mathbf{E}_{in} = \left(\frac{3}{\epsilon + 2}\right)\mathbf{E} \qquad (1)$$

In most metals, where $|\epsilon| \gg 1$, $|\mathbf{E}_{in}| \ll |\mathbf{E}|$ and the external field is screened from the interior of the sphere. However, for noble metals at optical frequencies, the field can be concentrated (anti-screened) inside. For example, for Ag at 380 nm, $\epsilon = -2 + 0.2i$ and the modulus of $(\epsilon + 2)$ goes nearly to zero. This resonance in the internal field produces a resonance in the Rayleigh scattering and absorption spectra, referred to as the "dipolar plasmon." The electromagnetic field $\mathbf{E}_S$ just above the surface along the direction of $\mathbf{E}$ is $\mathbf{E}_S = \epsilon\mathbf{E}_{in}$. The electromagnetic field is therefore enhanced both inside and outside the metallic sphere, with respect to the incident field intensity, $\mathbf{E}$.

$\mathbf{E}_{in}$ creates a coherently oscillating dipole $\mathbf{P}$ that scales in magnitude with a^3

$$\mathbf{P} = 4\pi\left(\frac{\epsilon - 1}{\epsilon + 2}\right)a^3\mathbf{E} \qquad (2)$$

where a is the radius of the particle (note that we use cgs units). The local field of $\mathbf{P}(\omega)$ creates the enhanced $\mathbf{E}_S$. In a dielectric material, $\mathbf{P}$ represents polarization of bound electrons. In a metal at the dipolar plasmon resonance, $\mathbf{P}$ is a coherent sum of electron−hole pairs oscillating along the direction of $\mathbf{E}$, and size quantized in the sphere.[24] Individual electron−hole pairs in the superposition have an energy difference that corresponds to the photon energy. These pairs cannot be characterized by a temperature; they are ballistic electron−hole pairs that have not dephased. $\mathbf{P}$ can re-radiate without energy loss at the frequency of the driving $\mathbf{E}$ field, or dephase by scattering and relaxation down to the Fermi level on a femtosecond time scale. The latter process corresponds to irreversible photon absorption yielding heat. To quote Kawabata and Kubo, "Thus, the plasma resonance can be considered as the free carrier absorption which is enhanced by a sort of anti-shielding at the frequency of the plasma mode."[24] Both local field enhancement and coherent, ballistic electron−hole pair oscillation are simply different aspects of the EM response of small metallic particles. If $\mathbf{P}$ is large, then $\mathbf{E}_S$ is enhanced.

$\mathbf{P}$ coherently sums the transition dipoles of individual electron−hole pairs. Dephasing and energy loss destroy this large dipole and create uncorrelated pairs that re-radiate only weakly. Therefore, metal particles do not normally show detectable Stokes shifted re-radiation. $\mathbf{P}$ can dephase by bulklike scattering processes. However, in crystalline Ag, the mean free path for a ballistic electron 1 eV above the Fermi surface is about 80 nm,[25] and the contribution of bulk dephasing to the plasmon width is small. In small particles, therefore, $\mathbf{P}$ dephases principally by surface scattering. This size quantization effect progressively broadens the plasmon resonance as a^{-1}.[24,26]

In an ~100 nm particle, $\mathbf{P}$ is a large transition dipole with an optical cross section of $\sim 10^{-10}$ cm^2. To explain the 10^{-14} cm^2 Raman cross section observed, $\mathbf{P}$ must be the optical transition that is coupled to the R6G vibrational modes. $\mathbf{P}$ can couple to an adsorbed molecule in two ways: (a) via the local field of $\mathbf{P}$ through an enhanced $\mathbf{E}_S$, or (b) by direct electron exchange, i.e., wave function overlap.

Interaction of Ballistic Electrons with Chemisorbed Molecules. Several experiments show that a ballistic electron or plasmon can interact strongly with chemisorbed molecules having low-lying LUMO levels. In Ag particles where the plasmon dephases principally via surface scattering, the dephasing rate w is given by $w \approx Cv_F/a$, in a semiclassical

(24) Kawabata, A.; Kubo, R. *J. Phys. Soc. Jpn.* **1966**, *21*, 1765−1772.
(25) Quinn, J. J. *Phys. Rev.* **1962**, *126*, 1453−1457.
(26) Kreibig, U.; Gartz, M.; Hilger, A. *Ber. Bunsen-Ges. Phys. Chem.* **1997**, *101*, 1593−1604.

approximation where v_F is the Fermi velocity. For a given radius a, w increases in the presence of chemisorbed molecules. For example, C is 4× larger for particles with chemisorbed CO than for bare particles.[26] The plasmon wave function decays principally by scattering from the chemisorbed CO, rather than by bulk or other surface processes. This scattering seems to occur by transient negative CO ion formation.[27]

In a vacuum, photodesorption of chemisorbed molecules on flat metal surfaces (e.g., NO on Pt) can occur by capture of ballistic ("hot") electrons into the LUMO orbital.[28] This electron capture yields a chemisorbed negative ion which can exist for femtoseconds before the electron tunnels back into the metal at a lower energy. This process results in a vibrationally excited neutral molecule which can subsequently either relax or desorb from the surface. Gadzuk has modeled the impulsive deposition of energy in the molecule and subsequent desorption by Gaussian vibrational wave packet dynamics in a fashion similar to time dependent resonant Raman theory.[29]

Other experiments further demonstrate the interaction between ballistic electrons in the metal and chemisorbed species. In low-temperature experiments, negative ions created by irradiation of a rough Ag substrate with adsorbed SERS active molecules have been trapped and detected.[30] Additionally, Otto and co-workers have systematically observed hot electron reactions with adsorbed species on rough Ag surfaces in electrochemical cells.[31] In these experiments, ballistic electrons were created by injection diodes and propagated across a 15 nm thick Ag film to the electrochemical interface.

Excitation of Ag Particle Plasmon Emission by Tunneling Electrons. While metal particles with clean surfaces normally do not luminesce, a Stokes shifted continuum emission is an integral aspect of SERS. This emission is similar to that observed in STM experiments from large Ag particles and rough Ag surfaces which luminesce with yields of 10^{-3} photons per tunneling electron.[32] Persson has modeled this phenomenon of STM-induced light emission as inelastic tunneling which excites a quantum of the plasmon.[33] The electron can couple with the plasmon $\mathbf{E_S}$ when it is in the barrier region between the STM tip and the particle. When inside the Ag particle, though, Persson's calculations predict that the "hot" electron has $\sim 10^3$ lower probability of plasmon excitation.

Once excited, a plasmon quantum in a small Ag particle decays primarily nonradiatively. Persson, though, has calculated that in a particle with $a \geq 30$ nm, the luminescence yield can reach 10% or more. This high probability of femtosecond time scale luminescence stems from the extremely large transition dipole $\mathbf{P}$ of large particles. It is related to the results of Mie theory, which show that for large particles ($a > 30$ nm), the Rayleigh scattering cross section is considerably larger than the photon absorption cross section. In other words, $\mathbf{P}$ re-radiates faster than the pairs can relax down to the Fermi surface, while for small particles, the reverse is true.

In electrochemical experiments, Otto and co-workers have also observed plasmon luminescence from rough Ag surfaces excited by ballistic electrons striking the surface from inside the metal. This emission is enhanced by chemisorbed species that donate charge into the metal surface. If one considers microscopic reversibility in regard to this experiment, then it would seem that a chemisorbed molecule could cause a radiative surface plasmon to decay by creating a ballistic electron inside the metal. This is, in fact, the mechanism in the Kreibig experiments.

Proposed Mechanism. Otto and co-workers have systematically explored the strong SERS that occurs for a number of chemisorbed molecules with low lying LUMOs on rough surfaces.[1] They qualitatively suggest that hot electrons generated in the metal transiently localize on the chemisorbed molecules, then tunnel back into the metal and subsequently emit. They also note that the strong inelastic continuum is associated with SERS. For R6G on Ag colloidal particles, Pettinger has quantitatively modeled a related idea; the entire plasmon (both electron and hole) transiently localizes on the molecule.[34] This later process is exchange coupled resonant energy transfer. Pettinger has also stressed the importance of a large Rayleigh cross section in enabling strong SERS.

In the large crystalline 100−200 nm particles in our study, the dominant $\mathbf{P}(\omega)$ decay mode must be radiative Rayleigh scattering. Yet, the prior literature teaches us that plasmons in crystalline Ag particles are also quite sensitive to dephasing by transient negative ion formation on chemisorbed molecules. We suggest that, most remarkably in these large particles, the plasmon can dephase by electron localization on just one chemisorbed R6G. When the electron tunnels back into the metal, it has some probability of inelastically exciting one real quantum of some lower energy plasmon of the complex particle, as suggested by the STM experiments and Persson's calculation. This lower energy plasmon emits with its full femtosecond radiative width. This broad emission may contribute to the broad underlying continuum in SERS. In this scheme, the lower energy plasmon is created by a sequential incoherent process, not a scattering process.

However, the R6G Raman lines appear to result from a scattering process rather than a sequential incoherent process. They have narrow line widths suggestive of ground state vibrational dephasing rates, as would be observed in molecular resonance Raman scattering from a strongly homogeneously broadened electronic state.[35] If the strong interaction between the chemisorbed molecule and $\mathbf{P}(\omega)$ is a function of the R6G normal modes, then vibrational modulation of the interaction creates a sideband $\mathbf{P}(\omega - \omega_{\mathbf{vib}})$ which can also radiate. In essence, resonance Raman scattering occurs, with $\mathbf{P}(\omega)$ as the resonant intermediate state. Formal theories of this sort have been discussed by Moskovits.[36]

The two states involved in the Raman scattering are $\mathbf{P}(\omega)$ and $\mathbf{P}(\omega - \omega_{\mathrm{vib}})$, the same states involved in the standard EM enhancement model. These states are coupled to the molecule by electron exchange, resulting in a larger effective cross section. It is remarkable that the cross sections are as large as have been measured; to our knowledge, such enhancements have not been predicted. Large particles are necessary in this SERS effect for two related reasons: (a) one quantum of $\mathbf{P}(\omega - \omega_{\mathrm{vib}})$ must have a significant probability of re-radiation, and (b) $\mathbf{P}(\omega)$ must have a large initial extinction cross section. $\mathbf{P}(\omega)$ is huge and necessarily has a fast femtosecond dephasing rate due to

(27) Persson, B. N. J. *Surf. Sci*. **1993**, *281*, 153−162.
(28) Gadzuk, J. W. in *Femtosecond Chemistry*; Manz, J., Wöste, L., Eds.; VCH Publishers: New York; 1995; pp 603−624.
(29) Lee, S. Y.; Heller, E. J. *J. Chem. Phys*. **1979**, *71*, 4777−4788.
(30) Feilchenfeld, H.; Chumanov, G.; Cotton, T. M. *J. Phys. Chem*. **1996**, *100*, 4937−4943.
(31) Otto, A. et al. In *Interfacial Science*; Roberts, M. W., Ed.; Blackwell Science: Oxford, 1997; pp 163−193.
(32) Gimzewski, J. K.; Sass, J. K.; Schlitter, R. R.; Schott, J. *Europhys. Lett*. **1989**, *8*, 435−440.
(33) Persson, B. N. J.; Baratoff, A. *Phys. Rev. Lett*. **1992**, *68*, 3224−3227.
(34) Pettinger, B. *J. Chem. Phys*. **1986**, *85*, 7442−7451.
(35) For a review of resonance Raman theory, see: Myers, A.; Mathies, R. In *Biological Applications of Raman Spectroscopy*; Spiro, T., Ed.; John Wiley & Sons: New York, 1987; Vol. 2, pp 1−58.
(36) See ref 2; sections V. B and V. C.

Rayleigh re-radiation, yet this state still appears to be sensitive to one chemisorbed molecule.

There must be a wide range of effective chemisorptive coupling of $\mathbf{P}(\omega)$ to the molecule, as evidenced by the wide range of Rayleigh to SERS ratios in Figure 10. It will be important to understand the microscopic nature of such selective chemisorption, and the possible additional role of electronic resonance in a molecule such as R6G. In this regard, Kim et al. report that the (nonresonant) SERS molecule pyridine, when adsorbed at 0.6 langmuir on rough Ag surfaces, lowers the work function by ~1.5 eV.[37] This is attributed to charge transfer from the N lone pair orbital to the metal. One such chemisorbed molecule would locally lower the work function and thus interact strongly with the plasmon.

(37) Kim, C. W.; Villagran, J. C.; Even, U.; Thompson, J. C. *J. Chem. Phys.* **1991**, *94*, 3974−3977.

Acknowledgment. We thank J. Trautman, T. D. Harris, J. Macklin, Al A. Efros, J. Tully, and T. Heinz for informative discussions. We also thank the W. M. Keck Foundation for a start-up grant at Columbia, and Bell Laboratories for apparatus donation. This research was supported under DOE Grant DE-FG02-98ER14861. Materials research facilities at Columbia University are supported under NSF MRSEC Grant DMR-98-09687. L.E.B. dedicates this article to the memory of R. H. Laudise. As a Director in Bell Laboratories, he built a materials chemistry research organization that was focused on innovation and intellectual rigor. As a colleague, Bob Laudise was a selfless and wise friend and a unique resource in solid state chemistry. His untimely death leaves an empty place in many lives.

JA992128Q